SYNTHESIS AND RED EMISSION OF Eu^{3+} DOPED $NaLaMo_2O_8$ PHOSPHORS [**]

J. Sun, Q. Li[*], Q. Zhou

Shandong Labor Vocational and Technical College,
Jinan 250022, China; e-mail: fdwanlei@yeah.net

Eu^{3+} doped $NaLaMo_2O_8$ phosphors were synthesized by a conventional solid state reaction. The phase and luminescent properties of the synthesized phosphors were investigated in the current work. In $NaLaMo_2O_8$, Eu^{3+} ions replace La^{3+} ions and form solid compound. This substitution induces the 2θ angles of diffraction peaks to shift to larger values. Under excitation at 395 nm, $NaLaMo_2O_8:Eu^{3+}$ phosphors exhibit emission bands in the range of 550–725 nm originating from $^5D_0 \rightarrow {}^7F_J$ transitions (J = 0, 1, 2, 3, 4) of Eu^{3+}. The strongest emission band corresponds to the $^5D_0 \rightarrow {}^7F_2$ transition, which indicates a site of Eu^{3+} without inversion symmetry in $NaLaMo_2O_8$. The Eu^{3+} concentration has obvious influence on the luminescent properties of $NaLaMo_2O_8:Eu^{3+}$ phosphors. $NaLaMo_2O_8$:6mol%Eu^{3+} has the strongest excitation and emission intensities.

Keywords: *$NaLaMo_2O_8:Eu^{3+}$, phosphors, luminescence.*

СИНТЕЗ И КРАСНОЕ ИЗЛУЧЕНИЕ ЛЮМИНОФОРА $NaLaMo_2O_8$, ЛЕГИРОВАННОГО Eu^{3+}

J. Sun, Q. Li[*], Q. Zhou

УДК 535.37

Шаньдунский профессионально-технический колледж,
Цзинань, 250022, Китай; e-mail: fdwanlei@yeah.net

(Поступила 20 марта 2019)

Люминофоры $NaLaMo_2O_8$, легированные Eu^{3+}, синтезированы с помощью обычной твердофазной реакции. Исследованы фазовые и люминесцентные свойства синтезированных люминофоров. В люминофоре $NaLaMo_2O_8$ ионы Eu^{3+} заменяют ионы La^{3+} и образуют твердое соединение. Эта замена приводит к тому, что углы 2θ дифракционных пиков смещаются к большим значениям. При возбуждении λ = 395 нм люминофоры $NaLaMo_2O_8:Eu^{3+}$ демонстрируют полосы излучения в диапазоне 550–725 нм, возникающие в Eu^{3+} при переходах $^5D_0 \rightarrow {}^7F_J$ (J = 0, 1, 2, 3, 4). Самая сильная полоса излучения соответствует переходу $^5D_0 \rightarrow {}^7F_2$, что указывает на отсутствие инверсионной симметрии в $NaLaMo_2O_8$ относительно местоположения Eu^{3+}. Концентрация Eu^{3+} оказывает очевидное влияние на люминесцентные свойства люминофоров $NaLaMo_2O_8:Eu^{3+}$. Для $NaLaMo_2O_8$:6 моль% Eu^{3+} наблюдаются самые сильные интенсивности возбуждения и излучения.

Ключевые слова: *$NaLaMo_2O_8:Eu^{3+}$, люминофоры, люминесценция.*

Introduction. There has been a steady increase in theoretical and experimental studies of lanthanide-activated inorganic phosphors over the past decade due to an ever-increasing demand for photoluminescence and related applications, such as lighting, electronic display, lasing, anti-counterfeiting, biological labeling, and imaging [1]. The lanthanide-activated inorganic phosphors offer better photo stability and improved color performance in the form of higher monochromatic (color) purity and spatial resolution. Moreover, these inorganic phosphors present wide optical tunability over emission wavelength and lifetime, as enabled by the intra-configurational 4*f*–4*f* and inter-configurational 4*f*–5*d* transitions of lanthanides [2, 3]. In the field of

[**] Full text is published in JAS V. 87, No. 4 (http://springer.com/journal/10812) and in electronic version of ZhPS V. 87, No. 4 (http://www.elibrary.ru/title_about.asp?id=7318; sales@elibrary.ru).

white light emitting diodes (WLEDs), lanthanide-activated inorganic phosphors are widely used and they are the critical parts of WLEDs [4]. WLEDs comprising inorganic phosphors have been regarded as third-generation solid state lighting devices due to their advantages compared with traditional incandescent and fluorescent lamps, such as high efficiency, low consumption of energy, long operating lifetime, fast switching, and low production cost [5, 6].

Compounds of the rare earth tungstate and molybdate have a long history of practical applications due to their unique luminescence properties originating from the electron transitions within the 4*f* shell [7]. As is known, the luminescence of doped rare earth tungstate/molybdate is one of their most important properties. They are promising candidates for WLEDs because they are good hosts for lanthanide ions and can yield white light in combination with the narrow-line emission of doped lanthanide ions. Trivalent europium ion (Eu^{3+}) is well known as a red-emitting activator due to its $^5D_0 \rightarrow {}^7F_J$ transitions (J = 0, 1, 2, 3, 4). In addition to the above emission bands, other emission bands originating from higher ^5D levels, such as $^5D_1$ (green), $^5D_2$ (green and blue), and $^5D_3$ (blue), can probably be observed depending upon the host lattice (phonon frequency as well as the crystal structure) and the doping concentration of Eu^{3+}. Several of Eu^{3+} doped rare earth tungstate/molybdate materials have shown good potential as red phosphors in phosphor-converted WLEDs, such as $NaGd(WO_4):Tb^{3+}$ [8], $NaLa(WO_4)_2:Eu^{3+}/Li^+$ [9], $Na_5Eu(WO_4)_4:Bi^{3+}/Sm^{3+}$ [10], $NaY(WO_4)_2:Eu^{3+}$ [11], $(Na_{0.5}La_{0.5})MoO_4:Re^{3+}$ (RE = Eu, Tb, Dy) [12], $NaLa(MoO_4)_2:Sm^{3+}/Dy^{3+}$ [13], $NaY(MoO_4)_2:Eu^{3+}$ [14], $LiLn(MO_4)$ (Ln = La, Eu, Gd, Y, M = W, Mo) [15], and $LiLaMo_2O_8:Eu^{3+}/Bi^{3+}/Sm^{3+}$ [16].

$NaLaMo_2O_8$ belongs to the family of double molybdate compounds and has attracted a tremendous amount of attention because of the excellent thermal and chemical stabilities and the good absorption and emission cross-sections of rare earth ions in their lattices [17]. $NaLaMo_2O_8$ has a structure similar to the scheelite $CaWO_4$ and has a number of attractive features due to the low symmetry of the crystal lattice [18]. In $NaLaMo_2O_8$ crystal lattice, Mo^{6+} ion is coordinated by four O^{2-} ions in a tetrahedral symmetry, and Na^+ and La^{3+} cations are randomly distributed over the same sites, which are coordinated by eight O^{2-} ions from near four MoO_4^{2-} groups [19, 20]. The random distribution of La^{3+} is helpful for the inhomogeneous broadening of spectral bands when rare earth ions are doped into the crystal lattice and replace La^{3+} ions.

In this work, we report the synthesis and luminescence of Eu^{3+} doped $NaLaMo_2O_8$ phosphors. The influence of Eu^{3+} concentration on luminescent properties of $NaLaMo_2O_8:Eu^{3+}$ was investigated carefully.

Experimental. A series of $NaLaMo_2O_8$:*x* mol%Eu^{3+} (*x* = 2, 4, 6, and 8) phosphors was synthesized by a conventional solid state reaction. Na_2CO_3 (99.9%), La_2O_3 (99.9%), MoO_3 (99.9%), and Eu_2O_3 (99.99%) were used as raw materials in the synthesis of Eu^{3+} doped $NaLaMo_2O_8$ phosphors. The raw materials were purchased from the Aladdin Chemical Reagent Company in Shanghai, China. All of raw materials were used directly without further purification. In a typical synthesis, stoichiometric raw materials were weighed and ground in an agate mortar. Then the mixture was transferred into a crucible and calcined at 900ºC for 4 h in air. After the system cooled to room temperature, the product was ground again for the measurements.

The XRD patterns of the synthesized phosphors were measured by a Rigaku-Dmax 2500 diffractometer. The excitation and emission spectra were obtained by an Edinburgh Instrument FLS920 spectrophotometer equipped with a 150W xenon lamp as the excitation source.

Results and discussion. Figure 1 gives the XRD patterns of the synthesized phosphors and the standard data of JCPDs card No. 85–1751 (pure $NaLaMo_2O_8$). The sharp diffraction peaks in the XRD patterns indicate the excellent crystallinities of the Eu^{3+} doped $NaLaMo_2O_8$ phosphors. All of diffraction peaks agree well with the standard diffraction peaks of pure $NaLaMo_2O_8$, suggesting that the doped Eu^{3+} ions do not change the phase of the $NaLaMo_2O_8$ host. There are no diffraction peaks corresponding to impurity, which demonstrates the single phase of the synthesized phosphors. Due to the similar ionic radii between La^{3+} (1.160 Å, CN = 8) and Eu^{3+} (1.066 Å, CN = 8), Eu^{3+} ions replace La^{3+} sites in $NaLaMo_2O_8:Eu^{3+}$ phosphors. The 2θ angles of diffraction peaks shift to larger values for the synthesized $NaLaMo_2O_8:Eu^{3+}$ phosphors, which is induced by the smaller ionic radius of Eu^{3+} than that of La^{3+}. The detailed values of 2θ angles for JCPDs card No. 85-1751 and $NaLaMo_2O_8$:*x* mole % Eu^{3+} (*x* = 2, 4, 6, and 8) are provided in Table 1.

Figure 2 provides the excitation spectra of $NaLaMo_2O_8$:*x* mol% %Eu^{3+} (*x* = 2, 4, 6, and 8) phosphors when monitoring at 615 nm. All of excitation spectra consist of a broad excitation band in the range of 200–350 nm and several sharp excitation bands in the range of 350–500 nm. The broad band is a charge transfer band (CTB), which results from the $O^{2-} \rightarrow Mo^{6+}$ charge transfer transition (from the 2*p* orbitals of oxygen ligands to the 5*d* orbitals of molybdenum atoms in MoO_4^{2-} groups) and the electron transfer from the O^{2-} 2*p* orbit to the empty 4*f* orbital of Eu^{3+} [12]. The sharp excitation bands in the range of 350–500 nm can be attributed to intra-configurational *f–f* transitions within the (Eu^{3+}) $4f^6$ configuration [21, 22]. These excita-

tion bands result from transitions from ground state ($^7F_0$) to the Eu^{3+} upper excited states ($^5D_{2,3,4}$ and $L_{6,7}$), i.e., $^7F_0 \rightarrow {}^5D_4$ (361 nm), $^7F_0 \rightarrow {}^5L_7$ (381 nm), $^7F_0 \rightarrow {}^5L_6$ (394 nm), $^7F_0 \rightarrow {}^5D_3$ (415 nm), and $^7F_0 \rightarrow D_2$ (465 nm) transitions, respectively. The excitation intensity of CTB increases continuously with increasing Eu^{3+} concentration, which is induced by the increased $O^{2-} \rightarrow Eu^{3+}$ electron transfer with increasing Eu^{3+} concentration. The excitation intensities of *f–f* transitions increase with increasing Eu^{3+} concentration from 2 to 6 mol%, then decrease with the further increase in Eu^{3+} concentration due to concentration quenching.

TABLE 1. 2θ angles (degree) of Crystal Orientations for JCPDs Card No. 85-1751 and $NaLaMo_2O_8$:*x* mol% Eu^{3+} (*x* = 2, 4, 6, and 8)

Samples	Crystal orientations							
	112	004	200	204	220	116	312	224
JCPDs no. 85-1751	28.060	30.422	33.514	45.888	48.126	52.621	56.637	58.007
$NaLaMo_2O_8$:2mol%Eu^{3+}	28.066	30.427	33.520	45.895	48.131	52.627	56.643	58.013
$NaLaMo_2O_8$:4mol%Eu^{3+}	28.073	30.432	33.525	45.901	48.137	52.633	56.649	58.018
$NaLaMo_2O_8$:6mol%Eu^{3+}	28.082	30.478	33.531	45.907	48.142	52.638	56.655	58.024
$NaLaMo_2O_8$:8mol%Eu^{3+}	28.089	30.483	33.537	45.913	48.148	52.644	56.660	58.030

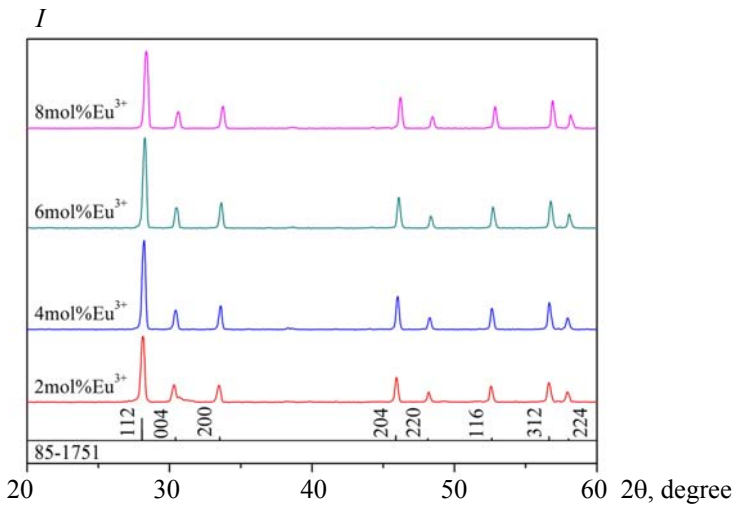

Fig. 1. XRD patterns of $NaLaMo_2O_8$:*x* mol% Eu^{3+} (*x* = 2, 4, 6, and 8) phosphors.

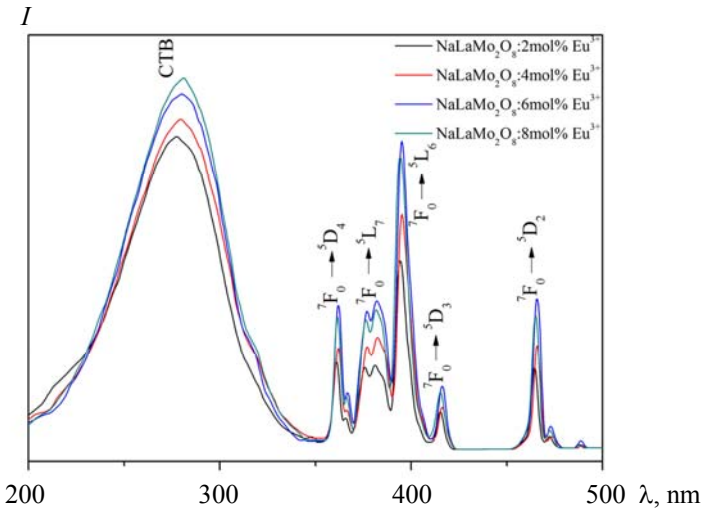

Fig. 2. Excitation spectra of $NaLaMo_2O_8$:*x* mol% Eu^{3+} (*x* = 2, 4, 6, and 8) phosphors.

Figure 3 exhibits the emission spectra of $NaLaMo_2O_8$:x mol% Eu^{3+} (x = 2, 4, 6, and 8) phosphors. Under excitation at 395 nm, all of phosphors exhibit emission bands originating from $^5D_0 \rightarrow {}^7F_J$ transitions (J = 0, 1, 2, 3, 4) of Eu^{3+}. The spectral shape and peak wavelength do not change with changing Eu^{3+} concentration, but the emission intensity increases with increasing Eu^{3+} concentration from 1 to 6 mol%, then decreases with further increase in Eu^{3+} concentration due to concentration quenching. In the emission bands originating from $^5D_0 \rightarrow {}^7F_J$ transitions (J = 0, 1, 2, 3, 4), the strongest one is the band coming from $^5D_0 \rightarrow {}^7F_2$ transition. For Eu^{3+}, the $^5D_0 \rightarrow {}^7F_1$ transition is a magnetic dipole transition, and the $^5D_0 \rightarrow {}^7F_2$ transition is an electric dipole transition [23]. From the Judd-Ofelt theory, it is known that the magnetic dipole transition is sensitive to the distortion at local chemical environment, but the electric dipole transition is highly sensitive to the surrounding coordination distortion. In the host lattice, occurrence of a predominant magnetic dipole transition or electric dipole transition is hence a strong indicator of whether the Eu^{3+} ion is occupying a site with inversion symmetry [24]. Specifically, the $^5D_0 \rightarrow {}^7F_2$ transition will become stronger if Eu^{3+} occupies a site without inversion symmetry, but the $^5D_0 \rightarrow {}^7F_1$ transition will dominate when Eu^{3+} ions occupy the sites with inversion symmetry. The strongest emission band coming from $^5D_0 \rightarrow {}^7F_2$ transition suggests the location of Eu^{3+} at a site without inversion symmetry.

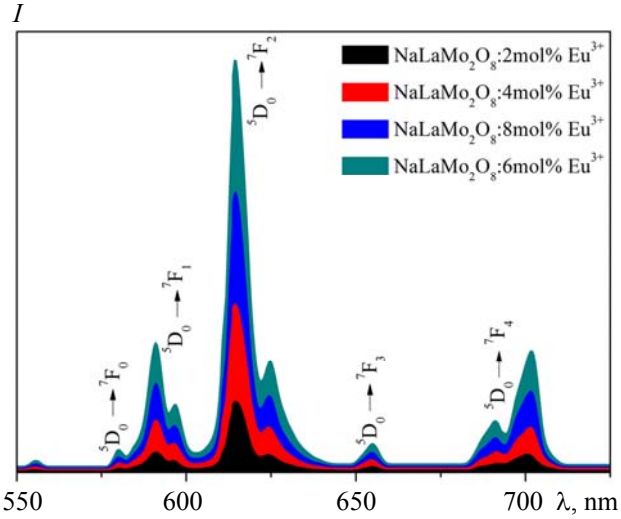

Fig. 3. Emission spectra of $NaLaMo_2O_8$:x mol% Eu^{3+} (x = 2, 4, 6, and 8) phosphors.

According to the Dexter's energy transfer theory, concentration quenching occurs as a result of the nonradiative energy migration among Eu^{3+} ions at high concentration [25]. The occurrence of nonradiative energy transfer may be caused by exchange interaction, radiation reabsorption, or multipole interaction [26]. The exchange interaction is a short-distance interaction, and the typical critical distance is about 5 Å. The mechanism of radiation reabsorption comes into effect only when there is a broad overlap between the emission spectrum of the sensitizer and the excitation spectrum of the activator. Based on the optimum doping concentration, the critical energy transfer distance (R_C) between Eu^{3+} ions in $NaLaMo_2O_8$ host is estimated by the formula of $R_C \approx 2(3V/4\pi X_C Z)^{1/3}$, where X_C is the critical concentration of Eu^{3+}, V is the volume of the unit cell, and Z is the number of cation sites in a unit cell [27]. For $NaLaMo_2O_8$:Eu^{3+} phosphors, V = 335.24 Å^3, Z = 2, and X_C = 0.06, and the critical transfer distance of Eu^{3+} in $NaLaMo_2O_8$ is calculated to be 47.474 Å. Therefore, the concentration quenching is induced by multipole interaction between neighboring Eu^{3+} ions.

Decay curves of $NaLaMo_2O_8$:x mol% Eu^{3+} (x = 2, 4, 6, and 8) phosphors at room temperature are shown in Fig. 4. The excitation wavelength is 395 nm and the monitoring wavelength is 615 nm. All decay curves can be fitted by a single-exponential decay model as the equation $I_t = I_0\exp(-t/\tau)$, where I_t is the emission intensity at time t; I is initial emission intensity, and τ is the decay time. The lifetimes of $NaLaMo_2O_8$:x mol% Eu^{3+} (x = 2, 4, 6, and 8) phosphors are 1.53, 1.39, 1.16, and 1.05 ms, respectively. It can be seen that the lifetime decreases in turn with increase in Eu^{3+} concentration from 2 to 8 mol%. The decreasing lifetime is induced by the increasing nonradiative transition [28].

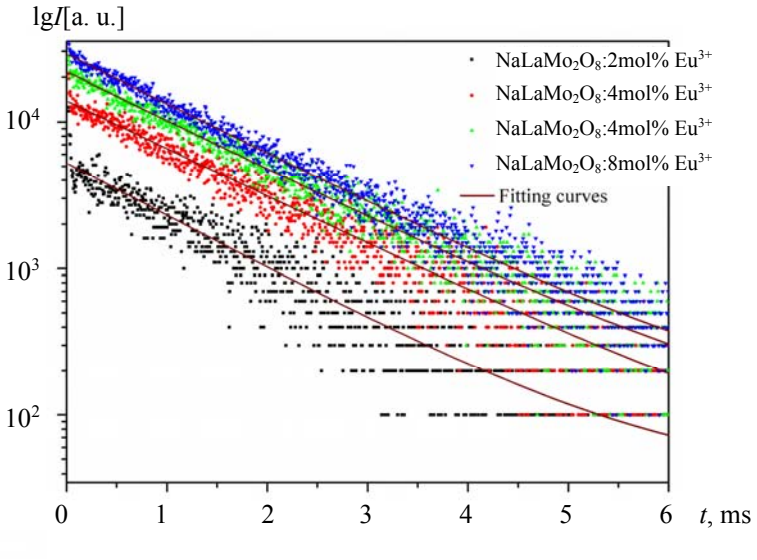

Fig. 4. Decay curves of $NaLaMo_2O_8$:*x* mol% Eu^{3+} (*x* = 2, 4, 6, and 8) phosphors.

Conclusions. We synthesized a series of Eu^{3+} doped $NaLaMo_2O_8$ phosphors by a conventional solids state reaction. The doped Eu^{3+} ions replace La^{3+} ions and do not change the phase of $NaLaMo_2O_8$ host. Upon excitation at 395 nm, emission bands resulting from $^5D_0 \rightarrow {}^7F_J$ transitions (J = 0, 1, 2, 3, 4) are exhibited. The stronger emission band corresponding to $^5D_0 \rightarrow {}^7F_2$ transition suggests a Eu^{3+} site without inversion symmetry in $NaLaMo_2O_8$. The luminescent properties of Eu^{3+} doped $NaLaMo_2O_8$ phosphors clearly depend on the Eu^{3+} concentration. When the Eu^{3+} doping concentration is 6 mol%, the highest emission intensity is obtained, and the lifetime of Eu^{3+} emission decreases in turn with increase in Eu^{3+} concentration.

REFERENCES

1. X. Qin, X. Liu, W. Huang, M. Bettinelli, X. Liu, *Chem. Rev.*, **117**, 4488–4527 (2017).
2. M. P. Hehlen, M. G. Brik, K. W. Krämer, *J. Lumin.*, **136**, 221–239 (2013).
3. L. van Pieterson, M. F. Reid, R. T. Wegh, A. Meijerink, *J. Lumin.*, **94-95**, 79–83 (2001).
4. M. Shang, C. Li, J. Lin, *Chem. Soc. Rev.*, **43**, 1372–1386 (2014).
5. Y. Yang, J. Li, B. Liu, Y. Zhang, X. Lv, L. Wei, X. Wang, J. Xu, H. Yu, Y. Hu, H. Zhang, L. Ma, J. Wang, *Chem. Phys. Lett.*, **685**, 89–94 (2017).
6. S. Mishra, R. Rajeswari, N. Vijayan, V. Shanker, M. K. Dalai, C. K. Jayasankar, S. S. Babu, D. Haranath, *J. Mater. Chem. C*, **1**, 5849–5855 (2013).
7. A. M. Kaczmarek, R. V. Deun, *Chem. Soc. Rev.*, **42**, 8835–8848 (2013).
8. Y. Liu, X. Yue, K. Cai, H. Deng, M. Zhang, *Energy*, **93**, 1413–1417 (2015).
9. Y. Liu, Z.-G. Lu, Y-Y. Gu, W. Li, *J. Lumin.*, **132**, 1220–1225 (2012).
10. D. Huang, Y. Zhou, W. Xu, Z. Yang, Z. Liu, M. Hong, Y. Lin, J. Yu, *J. Alloys Compd.*, **554**, 312–318 (2013).
11. Y. Tian, B. Chen, R. Hua, N. Yu, B. Liu, J. Sun, L. Cheng, H. Zhang, X. Li, J. Zhang, B. Tian, H. Zhong, *Cryst. Eng. Commun.*, **14**, 1760–1769 (2012).
12. B. Krishnan, J. Thirumalai, S. Thomas, M. Gowri, *J. Alloys Compd.,* **604**, 20–30 (2014).
13. L. Kong, X. Xiao, J. Yu, D. Mao, G. Lu, *J. Mater. Sci.*, **52**, 6310–6321 (2017).
14. J. Liu, B. Xu, C. Song, H. Luo, X. Zou, L. Han, X. Yu, *Cryst. Eng. Commun.*, **14**, 2936–2943 (2012).
15. Y. Liu, Y. Wang, L. Wang, Y. Y. Gu, S. H. Yu, Z. G. Lu, R. Sun, *RSC Adv.*, **4**, 4754–4762 (2014).
16. R. Cao, C. Liao, F. Xiao, G. Zheng, W. Hu, Y. Guo, X. Ye, *Dyes Pigments*, **149**, 574–580 (2018).
17. D. He, C. Guo, S. Zhou, L. Zhang, Z. Yang, C. Duan, M. Yin, *Cryst. Eng. Commun.*, **17**, 7745–7753 (2015).
18. T. Li, C. Guo, P. Zhao, L. Li, J. H. Jeong, *J. Am. Ceram. Soc.*, **96**, 1193–1197 (2013).
19. S. Brahma, R. N. P. Choudhary, A. K. Thakur, S. A. Shivashankar, *New J. Glass Ceram.*, **2**, 7–12 (2012).

20. L. Li, Y. Liu, R. Li, Z. Leng, S. Gan, *RSC Adv.*, **5**, 7049–7057 (2015).
21. Y. Yang, X. Wang, B. Liu, *Nano,* **9**, 1450008 (2014).
22. B. Liu, Y. Yang, X. Wang, *Nanosci. Nanotech. Lett.*, **5**, 1298–1301 (2013).
23. Y. Yang, *Mater. Sci. Eng. B*, **178**, 807–810 (2013).
24. S. G. Prasanna Kumara, R. Hari Krishna, N. Kottam, P. Krishna Murthy, C. Manjunatha, R. Preetham, C. Shivakumara, T. Thomas, *Dyes Pigments*, **150**, 306–314 (2018).
25. D. L. Dexter, J. H. Schulman, *J. Chem. Phys.* **22**, 1063–1070 (1954).
26. L. G. Van Uitert, *J. Electrochem. Soc.*, **114**, 1048–1053 (1967).
27. R. Yu, S. Zhong, N. Xue, H. Li, H. Ma, *Dalton Tran.*, **43**, 10969–10976 (2014).
28. Y. Chang, Z. Shi, Y. Tsai, S. Wu, H. Chen, *Opt. Mater.*, **33**, 375–380 (2011).